JETIR.ORG ISSN: 2349-5162 | ESTD Year : 2014 | Monthly Issue
JOURNAL OF EMERGING TECHNOLOGIES AND INNOVATIVE RESEARCH (JETIR)
An International Scholarly Open Access, Peer-reviewed, Refereed Journal

An Ensemble Models-based Parkinson's Disease Diagnosis Using Feature Selection and Improved Pelican Optimization Algorithm

N. Navaneetha[1], T. Suresh[2]

1 Research Scholar, Department of CSE, Annamalai University, Chidambaram, Tamil Nadu, India.

2 Associate Professor, Department of CSE, Annamalai University, Chidambaram, Tamil Nadu, India.

Abstract

Parkinson's disease (PD) affects people's movement, comprising changes in speech, writing ability, tremors, and stiffness in muscles. The PD's important levels are quite dangerous as the patients become more and more severe outcomes in the incapability of walking or standing. Initial identification accompanied by correct medicine can lessen the tremors and discrepancy signs for patients, allowing them to lead an ordinary life. In the area of the healthcare industry, Machine learning (ML) and deep learning (DL) are being constantly applied to a kind of data condition, containing handwritten patterns and acoustic voice recording for PD diagnosis. This manuscript presents an Ensemble Model-based Parkinson's Disease Diagnosis Using Feature Selection and Improved Pelican Optimization Algorithm (EMPDD-FSIPOA). This paper provides advanced deep learning and optimization algorithms for detecting PD in its early stages. Initially, the Z-score normalization has been used in the data pre-processing stage to transform input data into a beneficial design. For the feature selection (FS) method, the marriage in honey-bee optimizer (MBO) algorithm has been exploited. Furthermore, the proposed EMPDD-FSIPOA model executes ensemble of deep learning models namely variational autoencoder (VAE) method, temporal convolutional networks (TCN) model, and double deep Q networks (DDQN) technique for the classification process. At last, the parameter tuning process is performed through improved pelican optimization algorithm (IPOA) for developing the classification performance of the ensemble classifiers. The experimental assessment of the EMPDD-FSIPOA can be examined on a benchmark database. The widespread outcomes highlight the significant solution of the EMPDD-FSIPOA approach to the Parkinson's disease classification process.

Keywords: Ensemble Models; Parkinson's disease Diagnosis; Feature Selection; Improved Pelican Optimization Algorithm; Data Preprocessing

1. Introduction

The human brain is major computing component of human body, and if there is any small accident in any part of human body, before it will quickly influence the other organs [1]. One of silent impacts is Parkinson's disease (PD). It is general neurological disorder for affects movement of muscles in body. It impacts speech, mobility, and posture resulting in muscle rigidity, bradykinesia, and tremors. It arises owing to the death of neurons and leads to reduction of dopamine stages in the brain [2]. The lower level of dopamine hamper communication among connections, producing ineffectual function of motor. The physical indications are movement complications along with shaking, slowness, and rigidity [3]. Whereas, the psychological indications contain dementia, depression, and emotional concerns [4]. PD has five levels of development and ninety percent of PWP shows indications of vocal cord damage as indicated in level zero. Common voice modulation signs contain dysarthria and dysphonia [5].

Dysphonia might be described as the inability of the speaker to create a normal phonation owing to the method of phonatory impaired functioning, while dysarthria is more dependent on concerns with articulation while pronouncing words [6]. Particularly, hypokinetic dysarthria is related to reduction of articulation amplitude and loudness, a slow speech rate is incorporated with rushes of fast speech sometimes, and reduction of understanding ability [7]. Accurate and early analysis of PD is vital for many reasons: timely treatment, evasion of unnecessary therapies, and analysis connected to side effects, safety risks, and economic costs. Precise diagnosis is also crucial for patients being enlisted for medical trials. In recent times, to examine the development of this illness, multiple speech experiments have been organized [8]. DL and ML-based models are being employed on various data modalities together with handwritten patterns and acoustic voice recording for the examination of PD [9]. With the assistance of DL and ML approaches, we can identify the suitable features that are not conventionally implemented in the analysis of PD and based on these alternate signs recognize PD in its pre-clinical levels [10].

This paper presents an Ensemble Model-based Parkinson's Disease Diagnosis Using Feature Selection and Improved Pelican Optimization Algorithm (EMPDD-FSIPOA). Initially, the Z-score normalization has been used to transform input data. For the FS method, the marriage in honey-bee optimizer (MBO) algorithm has been exploited. Furthermore, the proposed EMPDD-FSIPOA model executes ensemble of DL models namely variational autoencoder (VAE) method, temporal convolutional networks (TCN) model, and double deep Q networks (DDQN) technique for the classification process. At last, the parameter tuning process is performed through improved pelican optimization algorithm (IPOA). The experimental assessment of the EMPDD-FSIPOA can be examined on a benchmark database.

2. Literature Works

Huang et al. [11] introduced a method able to precisely forecast PD levels, a multi-class classification task. This method utilized the overall 3D brain images as input and investigated with multiple model structures. Primarily, this work handled the 3D images are arrangements of 2D slices and fed them sequentially into 2D-CNN techniques pre-trained on ImageNet. Moreover, an attention mechanism is integrated to differ significance of diverse slices in the process of prediction. In [12], dual hybrid DNN that associates CNN with LSTM is projected

to analyze Parkinson's illness employing EEG signals, over the development of series and parallel integrated methods. The DCNN methods are employed to attain the essential aspects of ECG signals and remove significant data from them, after that the signals are sent through LSTM system to remove the dependency on features.

Abbasi and Rezaee [13] projected an innovative model for recognizing FoG events that depend on movement signals. For improving efficacy, an innovative structure incorporating a bottleneck attention module into a standard BiLSTM is projected. This framework is flexible to convolution bottleneck attention-BiLSTM (CBA-BiLSTM) and classifies signals employing data from leg, trunk, and ankle sensors. This method also decreases computational complication in dual stages: For choosing optimum channels over ensemble learning succeeded by reducing features employing attention mapping. Dharani and Thamilselvan [14] developed the chronological smart sunflower optimizer Algorithm (CSSFOA) for categorizing the PD from voice signal and voice data instances. The choice of optimum features is performed by the CSFOA. Yu et al. [15] developed a model for forecasting Parkinson's illness utilizing differential gut microbiota, called the Parkinson Gut Prediction Method (PGPM). A pre-processing model named CRFS was developed for FS. Subsequently, the projected LSIM method is employed for categorizing Parkinson's patients.

Agrawal and Sahu [16] projected a hybrid technique that integrates approaches for feature extraction and data augmentation with pre-trained CNN, and FS utilizing classification and optimization with the assistance of ML to improve identification of PD. In this study, primarily each kind of handwriting image is fed into 6 diverse pre-trained CNN methods and fine-tuned for classifying VGG16 structure giving a higher performance than the others. In another phase, the Binary grey wolf optimizer (BGWO) is employed for choice of optimum subset of features extracted from VGG-16 system by freezing the layers. In [17], a more generalized method is projected for recognition of PD in field of adaptation and self-supervised learning. This approach employs HuBERT, a huge deep neural network initially trained for recognition of speech, and trains it on unlabeled speech data from a population, which is related to the target group in self-supervised method. This technique is adapted and fine-tuned for utilization through diverse databases in several languages.

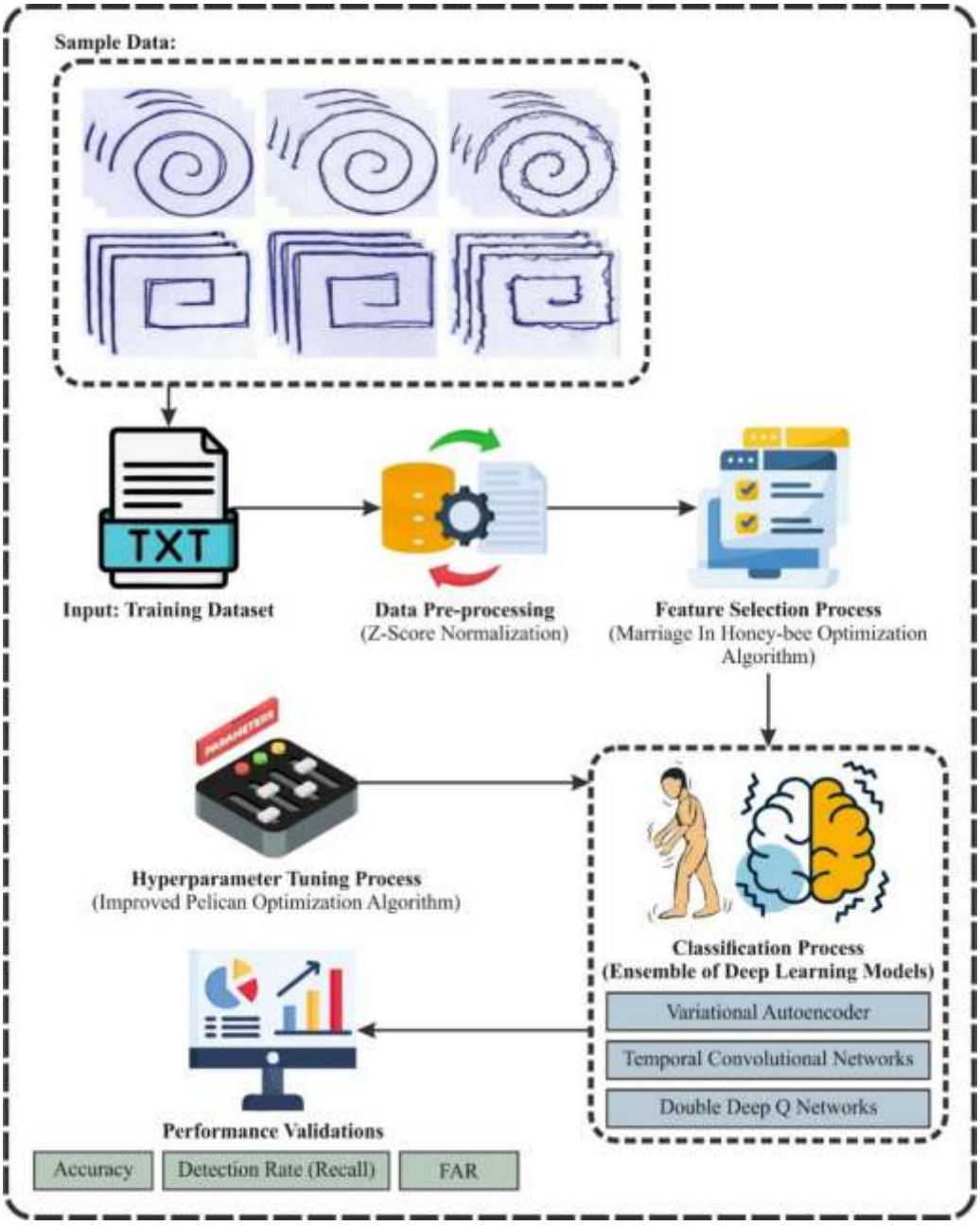

Fig. 1. Overall flow of EMPDD-FSIPOA system

3. The Proposed Model

In this paper, we have been presented an EMPDD-FSIPOA methodology. This paper provides advanced DL and optimization algorithms for detecting PD in its early stages. To accomplish that, the EMPDD-FSIPOA model contains data z-score normalization, an MBO-based FS process, ensemble of disease classification models, and parameter selection. Fig. 1 depicts the entire flow of EMPDD-FSIPOA system.

3.1. Data Normalization

Initially, the Z-score normalization has been used to transform input data into a beneficial design. Z-score normalization converts all features having a standard deviation (SD) of 1 and a mean of 0 [18]:

$$\tilde{x}_{t,j} = \frac{x_{t,j} - \mu_j}{\sigma_j} \quad (1)$$

Whereas σ_j and μ_j represents standard deviation and mean of feature j. This model is advantageous after data follows a Gaussian distribution.

3.2. MBO based Feature Selection

For the FS method, the MBO algorithm has been exploited. The MBO meta-heuristic was presented in this paper [19]. It is stimulated by the social mating behavior in bee populations. It is a developmental model established for solving composite combinational difficulties. MBO utilizes tactics derived from search for adjacent solutions, situating it among similar classes as GAs and ant colony optimization. The bee mating modeling for optimizer problem-solving is established, in this paper. Bee colonies contain queens, workers, offspring, and drones. The method starts with the nuptial fight of the queen, however, she mates with numerous drones. Primarily a queen bee's type species is arbitrarily produced. Worker bees, performing as local search heuristic, increase this primary solution. Then, the queen undertakes numerous pair-off fights. All fights include the arbitrary initialization of the queen's speed and energy. Productive mating, established by features namely the drone's fitness and the queen's energy, leads to the genetic matter of the drone being collected in the queen's sperm sac. Later all fights, the queen produces novel young by integrating her genetic matter with arbitrarily picked material from the sperm container. All processes are important for the performance of the model in discovering best solutions. This method utilizes a clean exploration approach, undertaking numerous queen routes as promising. All queens are primarily given random speed S_0 and energy E_0 values amongst 1.0 and 0.5 to enable an average of 717 matings per fight. Throughout the fight, the queen's speed and energy reduce based on Eqs. (2) and (3).

$$E(t+1) = E(t) - g \tag{2}$$

$$S(t+1) = \alpha \cdot S(t) \tag{3}$$

Whereas parameters g and α are similar to the lessening parameter of the queen's speed and energy at sample t, correspondingly.

Drones nearer the queen have a high mating likelihood as described by Eq. (4). These drones are specially picked for genetic reunion.

$$p(q,d) = mn\left\{1, e^{-\frac{l(q,d)}{s(t)}}\right\} \tag{4}$$

Whereas $l(q,d) = dist\big(f(q), f(d)\big)$ denotes distance among the assessments of the fitness functions of the drone and queen, and $s(t)$ signifies speed of the queen at sample t.

In MBO model, queen bees arbitrarily choose drones to mate. A drone can be recognized as a parent after its mating possibility surpasses randomly generated values among $(0, 1)$. one-half of the genetic matter of the drone is then combined into the queen's sperm sac, representing an effective mating. The mating fight ends after the energy of the queen declines, for example, $E(t) = 0$, or the sperm sac is occupied. After returning to the hive, the queen starts breeding by arbitrarily picking genetic stuff of the drone from her sperm container for crossbreeding. The residual broods are unwanted. The procedure repeats till the end conditions are encountered.

In this model, the aims are combined into a particular objective procedure like a pre-set weighting that recognizes all objective positions. In this study, we accept a fitness function (FF) that incorporates either FS objectives as subjected in Eq. (5).

$$Fitness(X) = \alpha \cdot E(X) + \beta * \left(1 - \frac{|R|}{|N|}\right) \quad (5)$$

However $Fitness(X)$ implies the fitness value of a subset X, $E(X)$ embodies the classifier error rate by employing the picked features in the subset X, $|R|$ and $|N|$ represents chosen feature counts and the original feature counts in the dataset consistently, α and β stands for weighting of the reduction ratio and the classification error, $\alpha \in [0,1]$ and $\beta = (1 - \alpha)$.

3.3. Ensemble of Disease Classification Models

Furthermore, the proposed EMPDD-FSIPOA model executes ensemble of DL models namely VAE method, TCN model, and DDQN technique for the classification process.

3.3.1. VAE Method

The decoder and encoder are dual elements of VAE [20]. The decoder generates novel data by sampling from the possible space once the encoder maps the input data into it. In VAE method, it is essential to constrain latent variables to obey certain distributions. VAE presents Kullback-Leibler (KL) divergence as an additional loss term that is enhanced by a method named stochastic gradient variable-DB Bayesian. The role of KL divergence is to evaluate the divergence among the possible spatial and pre-set simple distributions that are employed to standardize the possible space and make its distribution more consistent.

$$KL(q_\varphi(z|x)\|p_\theta(z|x)) = \int q_\varphi(z|x) \log \frac{q_\varphi(z|x)}{p_\theta(z|x)} dz \quad (6)$$

Here $q_\varphi(z|x)$ represents estimated distribution that the encoder learns, and a posteriori distribution is $p_\theta(z|x), \varphi$ and θ are the decoder and encoder parameters correspondingly.

The loss function is:

$$L(\theta, \varphi, x) = KL(q_\varphi(z|x)\|p_\theta(z)) - E_{C1\varphi((z1x)}(logp_\theta(z|x)) \quad (7)$$

There are dual elements to loss function. KL divergence is the primary element, whereas reconstruction error is secondary. During this paper, $z = \mu + \sigma \cdot \varepsilon, \varepsilon \sim N(0,1)$, then

$$KL(q_\varphi(z|x)\|p_\theta(z)) = -\frac{1}{2}\left(1 + log\sigma_j^2 - \sigma_j^2 - \mu_j^2\right) \quad (8)$$

σ_j and μ_j specifies variance and mean of j latent variable of the output of encoder, correspondingly.

The reconstruction error $L(x, \hat{x})$ is given below:

$$L(x, \hat{x}) = \sum_{j=1}^{J} (x_j - \hat{x}_j)^2 \quad (9)$$

x_j signifies the jth element of x. Next

$$L(\theta, \varphi, x) = -\frac{1}{2}\left(1 + log\sigma_j^2 - \sigma_j^2 - \mu_j^2\right) + \lambda \sum_{j=1}^{J} (x_j - \hat{x}_j)^2 \quad (10)$$

Here, λ represents the weight of $L(x, \hat{x})$. After a lot of experiments, we set λ to 0.0001. Fig. 2 represents the infrastructure of VAE.

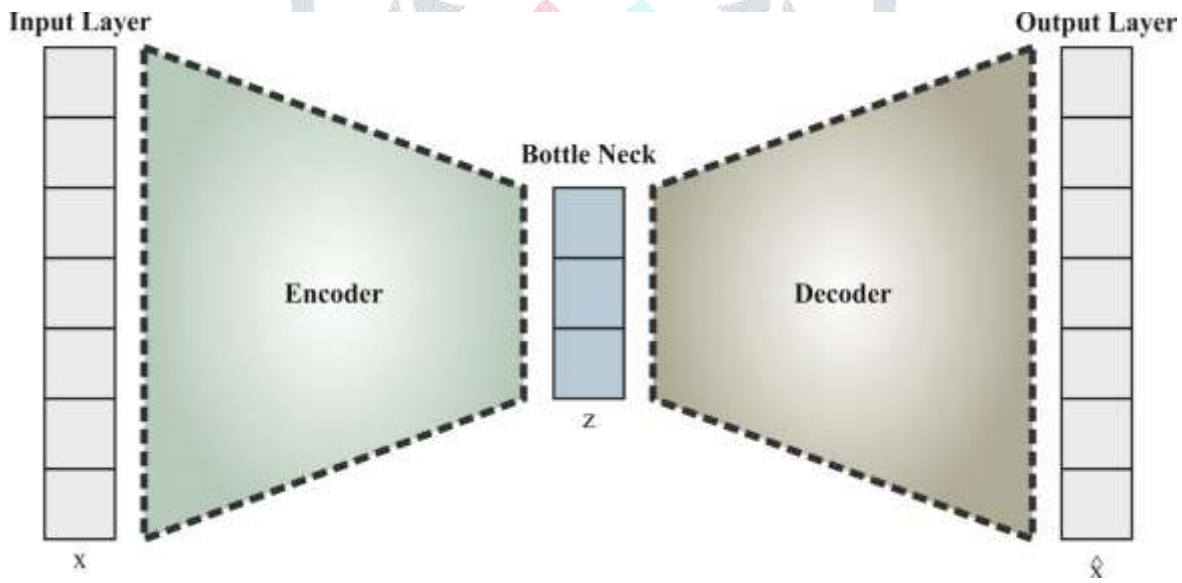

Fig. 2. VAE Structure

3.3.2. TCN Classifier

TCN uses residual connections and dilated causal convolutions to capture longer-term dependencies in sequential data [21]. TCNs are well-suited for time-series data since they may model temporal dependencies successfully. The structural design procedures input data over a series of temporal convolutional blocks, all designed for capturing various levels of temporal abstraction. These blocks are followed by global average pooling and classification through fully connected (FC) layers, permitting the network to make precise predictions according to the learned temporal features. TCNs provide the benefit of maintaining the sequence order and seizing long-range dependences deprived of the problem of gradient vanishing normally observed in conventional recurrent neural networks. The TCN block structure is described as:

Temporal Convolutional Block:

$$Block(x) = ReLU\left(Conv1D(x) + x_{downsampling}\right) \quad (11)$$

Temporal Convolutional Network (TCN):

$$TCN(x) = FC\left(GlobalAvgPool\left(Block(x)\right)\right) \quad (12)$$

This captures the sequential processing of input data over temporal convolutional blocks, followed by global average pooling and classification through FC layers.

3.3.3. DDQN Technique

DDQN was an enhanced technique dependent upon DQN, which intended mainly to resolve the issue of over-estimation of target Q-values in DQN [22]. The DDQN's main intention is to split action range from estimation of target Q-value by presenting a prediction and target networks for decreasing an estimation bias. Initially, the corresponding action $a_{\max}$ has been chosen over the prediction network $Q(s, a, \theta)$. The formulation is stated below:

$$a_{\max} = \text{argmax}_a Q(s_{t+1}, a, \theta) \quad (13)$$

Here, s_{t+1} denotes the state at $t + 1th$ time, a refers to an action taken, and θ means an online weight parameter of network.

The target Q-value computation depends upon the collaboration among prediction and target networks, and its mathematical formulation is given below:

$$y_i = r_{t+1} + \gamma Q[s_{t+1}, \text{argmax}_a Q(s_{t+1}, a, \theta_t \theta_t^-] \quad (14)$$

Where, r_{t+1} denotes an immediate reward attained by the agent afterward taking action a_t at time t; γ means a factor of discount, $\gamma \in [0,1Q[s_{t+1}, a, \theta_t]$ refers to Q-value estimation of taking action a at tth time in s_{t+1}, θ_t denotes the prediction network parameter at tth time, $\text{argmax}_a Q(s_{t+1}, a, \theta_t)$ signifies the highest Q-value between every action a in state s_{t+1} depend upon the parameters θ_t at tth time. $\theta_{\bar{t}}$ of the target network were upgraded by simulating the parameters θ_t of the network prediction; therefore, $\theta_t^- = \theta_t$. The agent interrelated and produced $(s_t, a_t, r_{t+1}, s_{t+1})$. The parameters of these networks were upgraded over the function of loss.

3.4. IPOA-based Parameter Selection

At last, the parameter tuning process is performed through IPOA to develop the classification performance of the ensemble classifiers. Despite conventional POAs having higher mining and exploration capabilities, they still confronted shortcomings regarding population diversity and robustness [23]. They are liable to drop into local ideals in the solution and search procedures that frequently result in stagnation within the population search. To enhance the performance of the algorithm, an advantage set is initially utilized for initializing the population of the pelican rather than arbitrary initialization. This distributes equally the searched grid into particular smaller areas, guaranteeing that all grids are completely searched which improves the population diversity and the algorithm's stability. Furthermore, the backward differential equation approach is presented to make reverse populations that enhance the complete population quality and stop the model from dropping into local bests. The reverse population generation is measured as demonstrated:

$$x_{ij} = \vartheta_j + rand \cdot (u_i - \vartheta_j) \quad (15)$$

Whereas x_{ij} signifies the $j\,th$-dimensional location of the $i\,th$ pelican; $i \in (1,p); j \in (1,q); p$ signifies the pelican population counts; q symbolizes the variable counts to be enhanced; and ϑ_j and u_j represent the lower and upper limitations of the $j\,th$ dimension to solve the problem, correspondingly. Afterward, every pelican has upgraded their locations, and the reverse solution for all individual populations is computed. At last, after the individual pelican attains novel locations and discovers solutions, it experiences crossover, mutation, and selection of the population. The novel individual is made utilizing the succeeding mutation processes:

$$z_i(k+1) = x_{r1}(k) + F * (x_{r2}(k) - x_{r3}(k)) \quad (16)$$

Whereas $x_{r1}, x_{r2},$ and x_{r3} signify 3 dissimilar k-generation individuals within the population. F represents the variation feature, and its value stands for randomly generated number inside [0,1]. The crossover process crossbreeds the changed individual $z_i(k+1)$ by the target one $x_i(k+1)$ to get the candidate individual of the objective one $u_i(k+1)$, as demonstrated:

$$u_i(k+1) = \begin{cases} z_i(k+1), rand \le CR \\ x_i(k+1), rand > CR \end{cases} \quad (17)$$

Here CR signifies a crossover feature inside [0,1]. The succeeding selection process equals the candidate fitness individual given that the targeted individual and next defines whether to substitute the targeted individual using candidate individuals within the following generation.

$$x_i(k+1) = \begin{cases} u_i(k+1), f(u_i(k+1)) \le f(x_i(k+1)) \\ x_i(k+1), f(u_i(k+1)) > f(x_i(k+1)) \end{cases} \quad (18)$$

Here f symbolizes the fitness function to solve the problem. Once the best individual drops into an extremely local, it will result in the model stagnating and converging.

The elite population targets to offer the additionally guaranteeing evolutionary direction, thus improving the local searching capability of the model.

$$x_i(k+1) = \begin{cases} x_{r1}(k) + F(x_{r2}(k) - x_{r3}(k)) \\ +F(x_{r4}(k) - x_{r5}(k)), rand(0,1) \le P \\ x_i^*(k) + F(x_{r2}(k) - x_{r3}(k)) \\ +F(x_{r4}(k) - x_{r5}(k)), else \end{cases} \quad (19)$$

Whereas $x_i(k+1)$ signifies the pelican's location in the $(k+1)\,th$ iteration; $x_i^*(k)$ represents the optimal pelican's location; $x_{r1}, x_{r2},$ and x_{r4} are arbitrarily chosen from the elite population; x_{r3} and x_{r5} are arbitrarily picked from the non-elite population. $rand(0,1)$ signifies randomly generated numbers inside [0,1]. P signifies the selection probability among dual mutation approaches and is computed as shown:

$$P = \frac{1}{1 + \exp\left(1 - \frac{\delta}{\beta}\right)} \tag{20}$$

Whereas δ and βrepresents maximum number and count of iterations, individually. At the start of the iterations, the model concentrates on improving the global searching capabilityAs a result, the model has an improved global optimizer capability in its initial phases. During this middle and future phases, the local searching capability of the model is improved and the rate of convergence is speeded up. To enhance the POA model, the arbitrary initialization is substituted with the fine point set initialization. Therefore, the POA performance is preserved and the solution quality is guaranteed. The IPOA mode originates a fitness function (FF) to reach boosted performance of classification. It outlines an optimistic number to embody the better outcome of the candidate solution. In this paper, the minimized of the classification ratio of error was reflected as FF. Its mathematical formulation is represented in Eq. (21).

$$fitness(x_i) = ClassifierErrorRate(x_i)$$
$$= \frac{no\ of\ misclassified\ samples}{Total\ no\ of\ samples} * 100 \tag{21}$$

4. Result Analysis and Discussion

The simulation validation of the EMPDD-FSIPOA technique is tested under four databases such as HandPD Spiral, Speech PD, HandPD Meander, and Voice PD.

Table 1 and Fig. 3 offer complete details of total and selected features. The HandPD Spiral database has 13 counts of features in total but only 3 features are selected. Where HandPD Meander database holds 13 total features but 4 features are only selected. While Speech PD database has 23 features but 5 features were selected. At last, Voice PD database selected only 4 features among 26 total number of features.

Table 1 Details of total vs selected features

Database	Total features	M-GOA	M-GWO	O-CFA	IFSODL	MBO-FS
HandPD Spiral	13	5	7	8	4	3
HandPD Meander	13	8	8	7	6	4
Speech PD	23	11	12	13	10	5
Voice PD	26	8	9	17	7	4

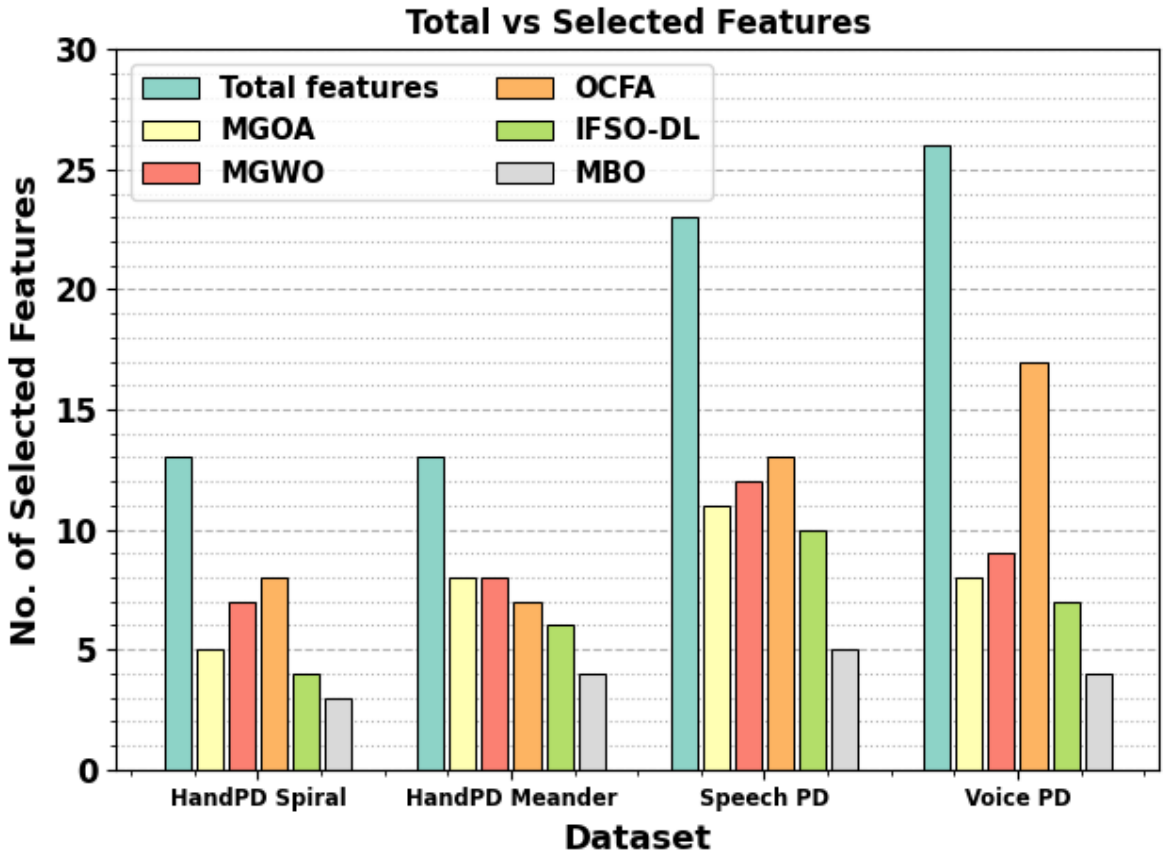

Fig. 3. Databases of total vs selected features

Table 2 established comparative results of EMPDD-FSIPOA technique on HandPD Spiral database with existing algorithms [24]. The table values specify that the proposed EMPDD-FSIPOA system has attained better performance with accuracy of 94.22%, detection rate of 98.89%, and FAR of 6.01 when compared to other existing algorithms such as M-GOARF, M-GOAKNN, M-GOADT, M-GWORF, M-GWOKNN, M-GWODT, and IFSODL.

Table 2 Comparative analysis of EMPDD-FSIPOA model on HandPD Spiral database

HandPD Spiral Database			
Methodologies	$Accu_y$	**Detection Rate**	**FAR**
M-GOAKNN	75.60	85.30	53.10
M-GOARF	92.90	97.90	21.90
M-GOADT	89.00	94.70	28.10
M-GWOKNN	73.40	81.90	50.00
M-GWORF	92.40	94.00	11.90
M-GWODT	92.40	94.00	11.90
IFSODL	93.30	98.20	8.00
EMPDD-FSIPOA	94.22	98.89	6.01

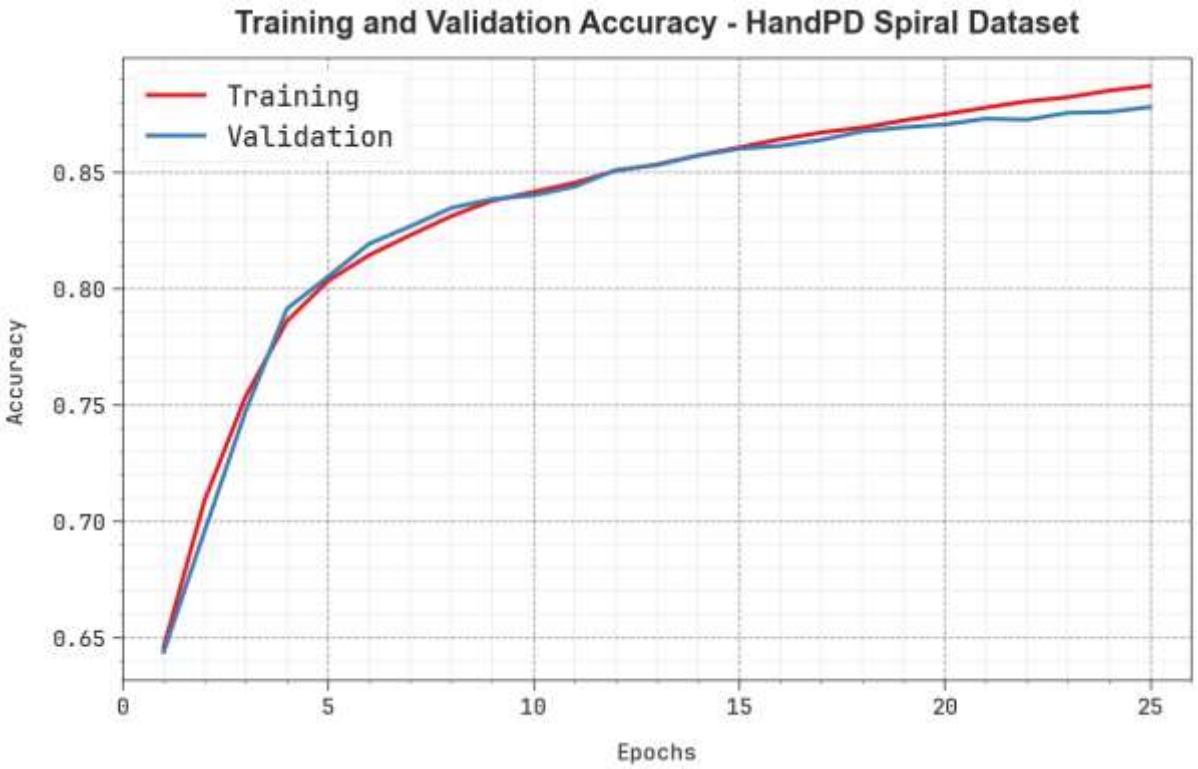

Fig. 4. $Accu_y$ curve of EMPDD-FSIPOA model on HandPD Spiral database

In Fig. 4, the training (TRA) $accu_y$ and validation (VAL) $accu_y$ results of the EMPDD-FSIPOA system on HandPD Spiral database are illustrated. The $accu_y$ analysis are calculated across the range of 0-25 epochs. The figure highlights that the TRA and VAL $accu_y$ analysis exhibitions a growing trend which notified the capacity of the EMPDD-FSIPOA with maximum outcomes across multiple iterations. Simultaneously, the TRA and VAL $accu_y$leftovers closer across the epochs, which identifies inferior overfitting and exhibits maximum outcomes of the EMPDD-FSIPOA technique, guaranteeing reliable prediction on unseen samples.

In Fig. 5, the TRA loss (TRALOS) and VAL loss (VALLOS) curves of the EMPDD-FSIPOA algorithm on HandPD Spiral database are shown. The values of loss are computed within the range of 0-25 epochs. It is suggested that the TRALOS and VALLOS analysis exemplify a diminishing tendency, informing the capacity of the EMPDD-FSIPOA system in balancing a trade-off between data fitting and simplification. The continuous reduction in values of loss besides assurances of the maximum outcomes of the EMPDD-FSIPOA approach and tuning the predictive outcomes over time.

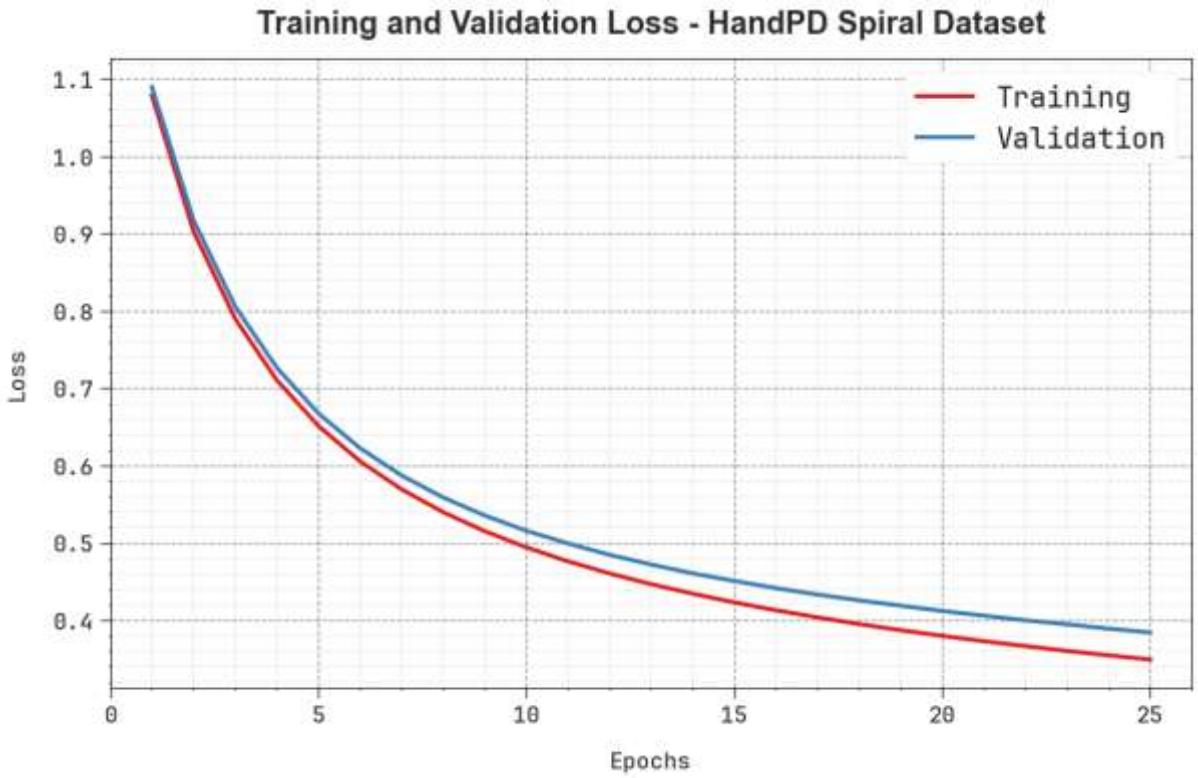

Fig. 5. Loss analysis of EMPDD-FSIPOA model under HandPD Spiral database

Table 3 offers comparative results of EMPDD-FSIPOA technique on HandPD Meander database with existing systems. The outcome stated that the EMPDD-FSIPOA methodology has proficient optimal performance. When compared to existing techniques namely M-GOARF, M-GOAKNN, M-GOADT, M-GWORF, M-GWOKNN, M-GWODT, and IFSODL, the proposed EMPDD-FSIPOA method has achieved higher performance with accuracy of 95.59%, detection rate of 98.87%, and FAR of 07.11.

Table 3 Comparative analysis of EMPDD-FSIPOA model on HandPD Meander database

HandPD Meander Database			
Methodologies	$Accu_y$	**Detection Rate**	**FAR**
M-GOAKNN	74.80	85.80	47.60
M-GOARF	93.70	97.89	19.10
M-GOADT	89.00	91.80	16.70
M-GWOKNN	72.80	85.80	60.00
M-GWORF	93.00	98.10	22.20
M-GWODT	88.00	92.00	22.20
IFSODL	94.00	95.23	13.50
EMPDD-FSIPOA	95.59	98.87	07.11

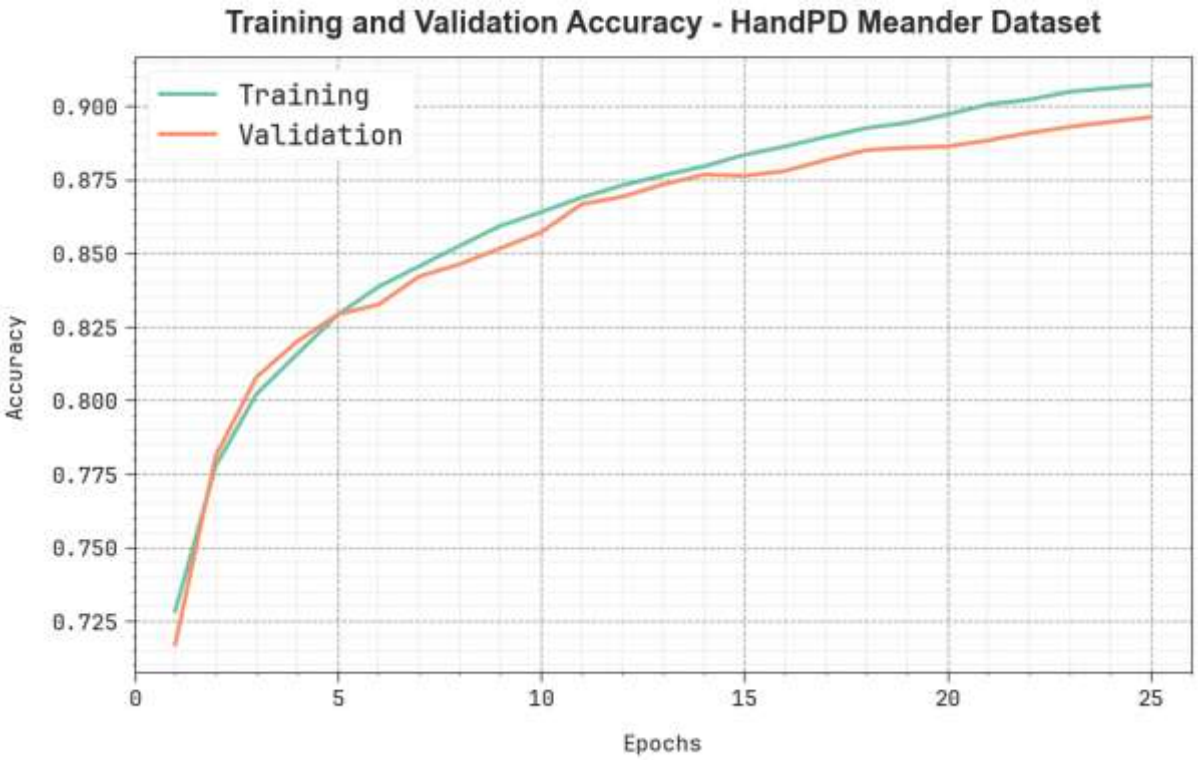

Fig. 6. $Accu_y$ curve of EMPDD-FSIPOA model on HandPD Meander database

In Fig. 6, the TRA $accu_y$ and VAL $accu_y$ analysis of the EMPDD-FSIPOA technique on HandPD Meander database is illustrated. The $accu_y$ analysis are computed across the range of 0-25 epochs. The outcomes highlighting that the TRA and VAL $accu_y$ analysis exhibitions an increasing trend which identified the capacity of the EMPDD-FSIPOA with higher solution across multiple iterations. Followed by, the TRA and VAL $accu_y$remains closer across the epochs, which directs inferior overfitting and exhibitions better performance of the EMPDD-FSIPOA technique, ensuring dependable prediction on unnoticed samples.

In Fig. 7, the TRALOS and VALLOS curve of the EMPDD-FSIPOA approach on HandPD Meander database is shown. The values of loss are computed within the range of 0-25 epochs. It meant that the TRALOS and VALLOS analysis exemplify a reducing tendency, informing the capacity of the EMPDD-FSIPOA in balancing a trade-off among simplification and data fitting. The continuous decrease in values of loss also assurances the maximal outcomes of the EMPDD-FSIPOA model and tunes the prediction outcomes over time.

Fig. 7. Loss curve of EMPDD-FSIPOA model on HandPD Meander database

The comparative performances of the EMPDD-FSIPOA technique on Speech PD database with existing models are exemplified in Table 4. When associated with existing algorithms such as M-GOAKNN, M-GOARF, M-GOADT, M-GWOKNN, M-GWORF, M-GWODT, and IFSODL, the proposed EMPDD-FSIPOA system has attained greater performance with accuracy, detection rate and FAR of 97.87%, 98.99%, and 9.08.

Table 4 Comparative analysis of EMPDD-FSIPOA technique on Speech PD database

Speech PD Database			
Methodologies	$Accu_y$	**Detection Rate**	**FAR**
M-GOAKNN	89.70	96.70	30.00
M-GOARF	94.90	97.67	22.20
M-GOADT	84.60	90.00	30.00
M-GWOKNN	91.80	97.40	30.00
M-GWORF	93.90	98.56	30.00
M-GWODT	89.80	94.90	30.00
IFSODL	95.30	96.32	18.50
EMPDD-FSIPOA	97.87	98.99	9.08

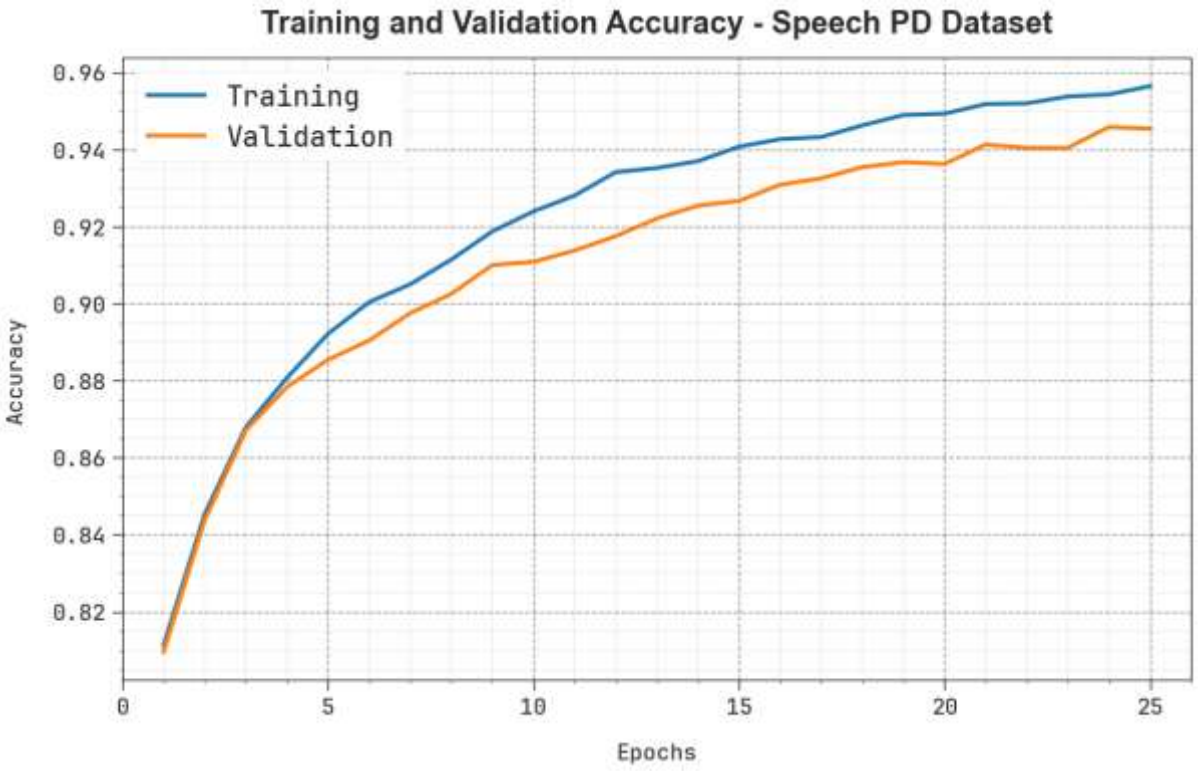

Fig. 8. $Accu_y$ curve of EMPDD-FSIPOA model on Speech PD database

In Fig. 8, the TRA $accu_y$ and VAL $accu_y$ performances of the EMPDD-FSIPOA approach on Speech PD database are depicted. The values of $accu_y$ are computed through a time period of 0-25 epochs. The figure underscored that the values of TRA and VAL $accu_y$ presents an increasing trend indicating the proficiency of the EMPDD-FSIPOA algorithm with maximum performance across multiple repetitions. In addition, the TRA and VAL $accu_y$ values remain close through the epochs, notifying decreased overfitting and expressing maximum outcome of the EMPDD-FSIPOA technique, which securities reliable calculation on unnoticed samples.

In Fig. 9, the TRALOS and VALLOS graph of the EMPDD-FSIPOA approach on Speech PD database is shown. The values of loss are computed through a time period of 0-25 epochs. It is exemplified that the values of TRALOS and VALLOS demonstrate a diminishing trend, which indicates the competency of the EMPDD-FSIPOA system in corresponding a tradeoff among data fitting as well as generalization. The consecutive dilution in values of loss also assurances the maximum outcome of the EMPDD-FSIPOA method and adjusts the calculation results gradually.

Fig. 9. Loss curve of EMPDD-FSIPOA model on Speech PD database

Table 5 delivers comparative study of EMPDD-FSIPOA technique on Voice PD database with existing methodologies. The performances imply that the proposed EMPDD-FSIPOA algorithm has reached better performance with accuracy of 98.95%, detection rate of 98.85%, and FAR of 08.46 when compared to existing models.

Table 5 Comparative analysis of the EMPDD-FSIPOA method on Voice PD database

Voice PD Database			
Methodologies	$Accu_y$	**Detection Rate**	**FAR**
M-GOAKNN	91.80	83.50	43.90
M-GOARF	95.70	95.40	32.00
M-GOADT	96.23	95.78	41.00
M-GWOKNN	85.80	80.30	28.10
M-GWORF	95.89	96.39	21.50
M-GWODT	97.01	98.14	28.19
IFSODL	98.24	97.80	17.31
EMPDD-FSIPOA	98.95	98.85	08.46

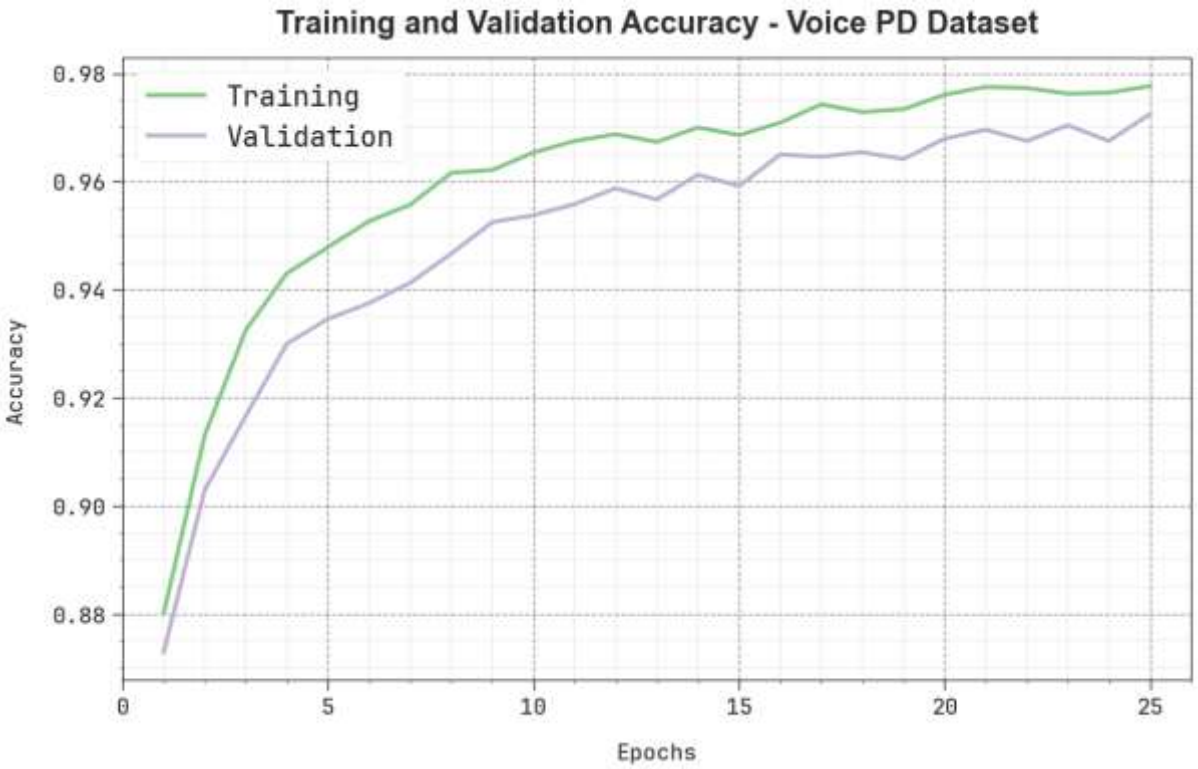

Fig. 10. $Accu_y$ curve of EMPDD-FSIPOA model on Voice PD database

In Fig. 10, the TRA $accu_y$ and VAL $accu_y$ performances of the EMPDD-FSIPOA technique on Voice PD database are showcased. The values of $accu_y$ are computed through a time period of 0-25 epochs. The figure underscored that the values of TRA and VAL $accu_y$ shows an increasing trend indicating the competency of the EMPDD-FSIPOA system with enhanced performance through multiple repetitions. Moreover, the TRA and VAL $accu_y$ values remain close across the epochs, notifying lesser overfitting and revealing improved outcomes of the EMPDD-FSIPOA method, which guarantees steady calculation on unnoticed samples.

In Fig. 11, the TRALOS and VALLOS graph of the EMPDD-FSIPOA approach on Voice PD database is shown. The values of loss are computed through a time period of 0-25 epochs. It is depicted that the values of TRALOS and VALLOS represent a declining tendency, which indicates the proficiency of the EMPDD-FSIPOA algorithm in harmonizing a tradeoff among data fitting as well as generalization. The succeeding dilution in outcomes of loss as well as securities the higher performance of the EMPDD-FSIPOA and alters the calculation solutions after a while.

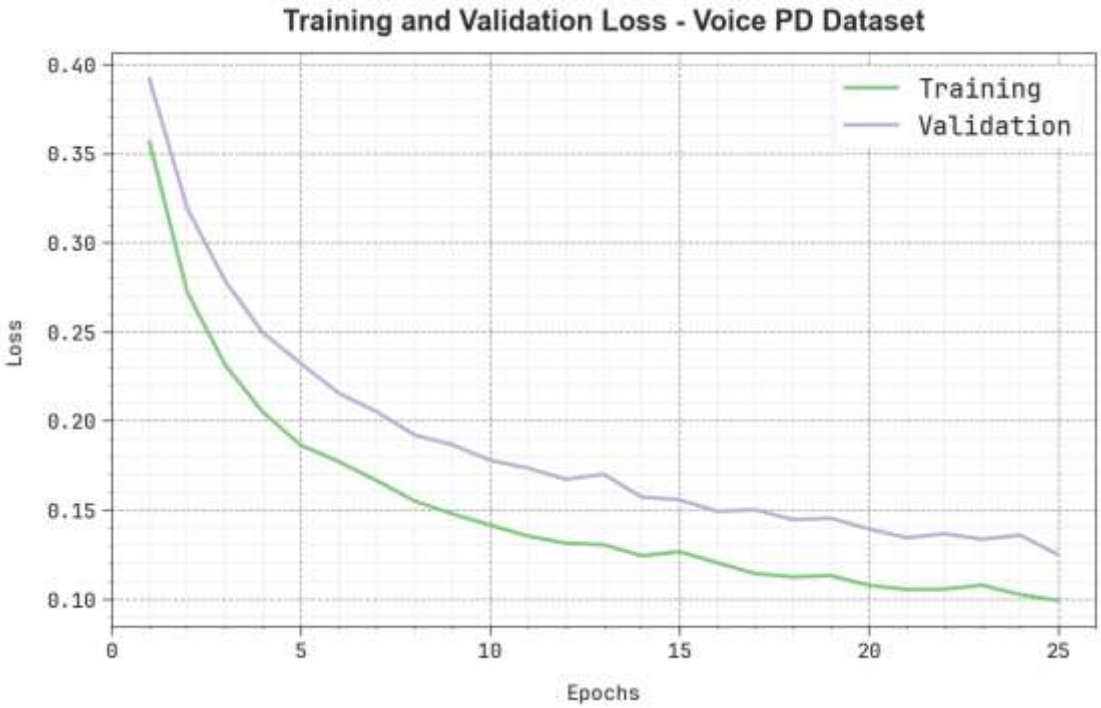

Fig. 11. Loss curve of EMPDD-FSIPOA model under Voice PD database

5. Conclusion

In this paper, we have been presented an EMPDD-FSIPOA methodology. This paper provides advanced DL and optimization algorithms for detecting PD in its early stages. To accomplish that, the EMPDD-FSIPOA model contains data z-score normalization, an MBO-based FS process, ensemble of disease classification models, and parameter selection. Initially, the Z-score normalization has been used to transform input data into a beneficial design. For the FS method, the MBO algorithm has been exploited. Furthermore, the proposed EMPDD-FSIPOA model executes ensemble of DL models namely VAE method, TCN model, and DDQN technique for the classification process. At last, the parameter tuning can be performed through IPOA to develop the classification performance of the ensemble classifiers. The experimental assessment of the EMPDD-FSIPOA can be examined on a benchmark database. The widespread outcomes highlight the significant solution of the EMPDD-FSIPOA approach to the Parkinson's disease classification process.

References

[1] Pahuja, G. and Nagabhushan, T.N., 2021. A comparative study of existing machine learning approaches for Parkinson's disease detection. *IETE Journal of Research*, *67*(1), pp.4-14.

[2] Govindu, A. and Palwe, S., 2023. Early detection of Parkinson's disease using machine learning. *Procedia Computer Science*, *218*, pp.249-261.

[3] Balaji, E., Brindha, D. and Balakrishnan, R., 2020. Supervised machine learning based gait classification system for early detection and stage classification of Parkinson's disease. *Applied Soft Computing*, *94*, p.106494.

[4] Rana, A., Dumka, A., Singh, R., Panda, M.K., Priyadarshi, N. and Twala, B., 2022. Imperative role of machine learning algorithm for detection of Parkinson's disease: review, challenges and recommendations. *Diagnostics*, *12*(8), p.2003.

[5] Oh, S.L., Hagiwara, Y., Raghavendra, U., Yuvaraj, R., Arunkumar, N., Murugappan, M. and Acharya, U.R., 2020. A deep learning approach for Parkinson's disease diagnosis from EEG signals. *Neural Computing and Applications*, *32*, pp.10927-10933.

[6] Khoury, N., Attal, F., Amirat, Y., Oukhellou, L. and Mohammed, S., 2019. Data-driven based approach to aid Parkinson's disease diagnosis. *Sensors*, *19*(2), p.242.

[7] Wodzinski, M., Skalski, A., Hemmerling, D., Orozco-Arroyave, J.R. and Nöth, E., 2019, July. Deep learning approach to Parkinson's disease detection using voice recordings and convolutional neural network dedicated to image classification. In *2019 41st annual international conference of the IEEE engineering in medicine and biology society (EMBC)* (pp. 717-720). IEEE.

[8] Mei, J., Desrosiers, C. and Frasnelli, J., 2021. Machine learning for the diagnosis of Parkinson's disease: a review of literature. *Frontiers in aging neuroscience*, *13*, p.633752.

[9] Wang, W., Lee, J., Harrou, F. and Sun, Y., 2020. Early detection of Parkinson's disease using deep learning and machine learning. *IEEE Access*, *8*, pp.147635-147646.

[10] Galarza, F.C., Lescano, L.F., Neri, L.E. and Nabieva, D., 2023. A Data Fusion Approach for Accurate Diagnosis of Parkinson's Disease. *Full Length Article*, *14*(1), pp.273-73.

[11] Huang, G.H., Lai, W.C., Chen, T.B., Hsu, C.C., Chen, H.Y., Wu, Y.C. and Yeh, L.R., 2025. Deep Convolutional Neural Networks on Multiclass Classification of Three-Dimensional Brain Images for Parkinson's Disease Stage Prediction. *Journal of Imaging Informatics in Medicine*, pp.1-17.

[12] Li, K., Ao, B., Wu, X., Wen, Q., Ul Haq, E. and Yin, J., 2024. Parkinson's disease detection and classification using EEG based on deep CNN-LSTM model. *Biotechnology and Genetic Engineering Reviews*, *40*(3), pp.2577-2596.

[13] Abbasi, S. and Rezaee, K., 2025. Deep Learning–Based Prediction of Freezing of Gait in Parkinson's Disease With the Ensemble Channel Selection Approach. *Brain and Behavior*, *15*(1), p.e70206.

[14] Dharani, M.K. and Thamilselvan, R., 2024. Hybrid optimization enabled deep learning model for Parkinson's disease classification. *The Imaging Science Journal*, *72*(2), pp.167-182.

[15] Yu, B., Zhang, H. and Zhang, M., 2025. Deep learning-based differential gut flora for prediction of Parkinson's. *PloS one*, *20*(1), p.e0310005.

[16] Agrawal, S. and Sahu, S.P., 2024. Image-based Parkinson disease detection using deep transfer learning and optimization algorithm. *International Journal of Information Technology*, *16*(2), pp.871-879.

[17] Siniukov, M., Xing, E., Isfahani, A. and Soleymani, M., 2025. Towards a Generalizable Speech Marker for Parkinson's Disease Diagnosis. *arXiv preprint arXiv:2501.03581*.

[18] Gupta, B.B., Gaurav, A., Attar, R.W., Arya, V., Bansal, S., Alhomoud, A. and Chui, K.T., 2024. Advance drought prediction through rainfall forecasting with hybrid deep learning model. *Scientific Reports*, *14*(1), pp.1-14.

[19] Palominos, P., Mazo, M., Fuertes, G. and Alfaro, M., 2025. An Improved Marriage in Honey-Bee Optimization Algorithm for Minimizing Earliness/Tardiness Penalties in Single-Machine Scheduling with a Restrictive Common Due Date. *Mathematics*, *13*(3), p.418.

[20] Zhang, L., Chen, B., Lyu, D., Wang, L. and Wang, K., Estimation of Lithium-Ion Battery Health State by Evae and Bigru Based on Eis. *Available at SSRN 5100808*.

[21] Chandankar, P. and Shetty, G., Human Activity Recognition (HAR): Overcoming Recognition's Curse of Normality in the Wild.

[22] Gao, J., Liu, N., Li, H., Li, Z., Xie, C. and Gou, Y., 2025. Reinforcement Learning Decision-Making for Autonomous Vehicles Based on Semantic Segmentation. *Applied Sciences*, *15*(3), p.1323.

[23] Wu, S., Cheng, X. and Li, H., 2025. sEMG Signal-Based Human Lower-Limb Intention Recognition Algorithm Using Improved Extreme Learning Machine. *Journal of Advanced Computational Intelligence and Intelligent Informatics*, *29*(1), pp.53-63.

[24] Bahaddad, A.A., Ragab, M., Ashary, E.B. and Khalil, E.M., 2022. Metaheuristics with Deep Learning-Enabled Parkinson's Disease Diagnosis and Classification Model. *Journal of Healthcare Engineering*, *2022*.